Intermetallics 142 (2022) 107444

Contents lists available at ScienceDirect

Intermetallics

journal homepage: www.elsevier.com/locate/intermet

Tensile mechanical properties of CoCrFeNiTiAl high entropy alloy via molecular dynamics simulations

Zhi Hui Sun [a], Jie Zhang [a], Gao Xin Xin [b], Lu Xie [a,*], Li Chun Yang [a], Qing Peng [c,**]

[a] School of Mechanical Engineering, University of Science and Technology Beijing, Beijing, 100083, PR China
[b] China Nuclear Power Technology Research Institute Co Ltd., Reactor Engineering and Safety Research Center, Shenzhen, 518031, China
[c] State Key Laboratory of Nonlinear Mechanics, Institute of Mechanics, Chinese Academy of Sciences, Beijing, 100190, China

ARTICLE INFO

Keywords:
High-entropy alloy
Tensile mechanical properties
Temperature effect
Molecular dynamics

ABSTRACT

High-entropy alloys (HEAs) are a new type of multi-principal metal materials that exhibit excellent mechanical properties, good thermal stability, and high corrosion resistance, with versatile potential applications. In this paper, we have investigated CoCrFeNi$(Al_{0.3}Ti_{0.2})_x$ HEA with different Ti and Al contents using XRD, tensile testing, and molecular dynamics simulations. The effects of Ti and Al contents and temperature on the mechanical properties were also explored. The experimental results showed that the CoCrFeNi$(Al_{0.3}Ti_{0.2})_x$ HEAs were mainly composed of the FCC matrix phase and γ' phase (Ni_3(Al, Ti)) after rolling and annealing. The addition of Ti and Al induced the formation of high-temperature strengthening phases in the CoCrFeNi HEA, which significantly improved the mechanical properties. The molecular dynamics simulations also indicates that the elastic modulus and tensile strength of CoCrFeNi$(Al_{0.3}Ti_{0.2})_x$ HEA are steadily improved with the Ti and Al addition. The tensile strength increases with the dislocation density. Besides, we have performed a high-temperature mechanical characterization of the CoCrFeNi$Al_{0.225}Ti_{0.15}$ HEA. The experimental data have revealed that the material's strength continuously declines with stretching temperature, opposed to that of toughness. The high-temperature tensile modulus of elasticity decreases with the temperature. Temperature also diminishes the tensile strength due to the average reduction of the dislocation density.

1. Introduction

High-entropy alloy (HEA) [1] is a new kind of equimolar multi-principal alloy. These unique materials go beyond the design of the traditional alloys with much richly design spaces. HEA are characterized by a particular atomic structure, which in turn stimulates the interaction of multiple microscopic mechanisms [2,3]. HEA exhibits various excellent macroscopic mechanical properties, such as high strength [1], superior hardness [4], high-temperature oxidation resistance, and good corrosion resistance [5]. Doping with different elements may cause a change in the structural and mechanical properties of HEAs. At the atomic scale, doping can change the atomic structure of HEA and aggregation of elements. The microstructural evolution caused by thermo-mechanical treatment may effectively improve the comprehensive mechanical properties [6]. The characteristics of multi-principal components provide a very high level of designability of HEAs. HEA significantly broadens the developmental horizons of new alloys and provides a possibility to surpass the performance limits of traditional alloys.

Many studies have been recently performed on HEAs' plasticity. Large blocks of HEA ingots have been prepared using different melting techniques, and the corresponding tensile properties were examined. Ma et al. [7] have prepared for the first time a single crystal FCC $Al_{0.3}$CoCrFeNi HEA with ⟨001⟩ orientation using the Bridgman directional solidification method. The tensile strength was only 399 MPa, but the total elongation could be as high as 80%. It is very challenging for the ⟨001⟩ orientation and the small-angle grain boundaries formed during the solidification process to suppress the slippage of dislocations during the stretching process effectively. Shun et al. [8] studied the microstructural and mechanical properties of the coarse-grained $Al_{0.3}$CoCrFeNi HEA after aging at 700 and 900 °C, showing that the aging treatment could promote the formation of hard precipitates to strengthen the alloy. However, due to the large grain size of the FCC matrix phase, the alloy's tensile strength after aging treatment was still

* Corresponding author.
** Corresponding author.
E-mail addresses: xielu@ustb.edu.cn (L. Xie), pengqing@imech.ac.cn (Q. Peng).

https://doi.org/10.1016/j.intermet.2021.107444
Received 12 September 2021; Received in revised form 20 November 2021; Accepted 17 December 2021
Available online 20 December 2021
0966-9795/© 2021 Elsevier Ltd. All rights reserved.

less than 600 MPa. He et al. [9] prepared a dispersion-strengthened HEA with nano-precipitated phases by adding Ti and Al as trace elements to FeCoNiCr alloy. The tensile test showed a significant work-hardening effect. The room temperature yield strength was 645 MPa, the breaking strength was more than 1 GPa, while the plastic elongation was 39%. Dong et al. [10] studied the effects of Co and Ni on the microstructural and mechanical properties of $AlCo_xCrFeNi_{3-x}$ eutectic-high-entropy alloys (EHEAs). They found that Ni and Co in the $AlCo_xCrFeNi_{3-x}$ EHEAs could replace each other, and that the (Ni + Co) atomic percentages of the FCC phase and B2 phase in each AlCoxCrFeNi$_{3-x}$ EHEAs was approximately equal. Besides, the $AlCo_xCrFeNi_{3-x}$ alloys with different Co、Ni content exhibited excellent and similar compression properties, with a fracture strength exceeding 2000 MPa and a compression rate above 35%.

Molecular Dynamics (MD) simulations is a powerful complementary approach to traditional theories and experimental methods [11]. For HEAs, it is of great significance to reveal and predict the properties at the atomic scale. Liu et al. [12] used MD simulations to study the mechanical behavior of AlCrFeCuNi HEA under uniaxial tensile load, and showed high strength and good plasticity. During tensile deformation, dislocation slip, lattice distortion, and twinning are still the main mechanisms of AlCrFeCuNi alloy plastic deformation. Afkham et al. [13] used the MD method to simulate the tensile behavior of $Al_xCrCoFeCuNi$ HEA at different temperatures. They studied the alloy's deformation behavior and mechanism at room temperature, high temperatures, and various strain rates. The yield stress decreased significantly with the temperature, while the alloy exhibited superplastic behavior under all test conditions; remarkably, the increment of Al content resulted in a significant decrease in the yield stress and elastic modulus. Korchuganov [14] studied mechanical properties of bulk $Co_{10}Cr_{10}Fe_{30}Mn_{30}Ni_{20}$ and $Co_{30}Cr_{30}Fe_{10}Mn_{10}Ni_{20}$ HEAs and determined Young's moduli of 81 and 103 GPa, respectively. Furthermore, it was found that in the process of high-rate stretching or compression, the plasticity in the single crystal CoCrFeMnNi was nucleated by the formation of internal accumulation faults. Qi et al. [15] studied the plastic deformation of single-crystal and polycrystalline CoCrFeMnNi HEA under tension and compression using the MD method and showed that the FCA/HCP phase transition occurred during the plastic deformation of HEA materials. At the same time, for compressive loading, the grains were refined, and the crystal orientation was different due to the interaction of inherent stacking faults (SFs) in different directions, which effectively improved the material's strength.

HEAs' excellent properties have sparked research interest. Extensive theoretical, experimental, and numerical studies have been performed. This paper aims to investigate the mechanical properties of CoCrFeNi $(Al_{0.3}Ti_{0.2})_x$ HEA (x = 0.25, 0.50, 0.75, 1.00) obtained by tensile experiments at room temperature and high temperatures. Furthermore, we used MD method to simulate the mechanical properties of CoCrFeNi $(Al_{0.3}Ti_{0.2})_x$ HEA under uniaxial tensile loading. The effects of temperature and Ti and Al contents on the mechanical properties were studied, and the dislocation changes during the stretching process were analyzed.

2. Experimental materials and methods

The composition of HEAs investigated in this paper was CoCrFeNi $(Al_{0.3}Ti_{0.2})_x$, where x = 0.25, 0.50, 0.75, 1.00. Experimental alloys were prepared in an arc melting furnace, and raw materials were high-purity (≥99.9%) Co, Cr, Fe, Ni, Ti, and Al metals. To prevent segregation of the alloy components, melting the master alloys was repeated four times to finally obtain oblate alloy ingots with a maximum diameter of about 38 mm and a thickness of about 12 mm.

From the maximum outer diameter of the cast samples, we cut out a sheet with a thickness of 3 mm, which was then subjected to heat treatment and rolling process. To eliminate the alloys' casting stress, we placed all the alloy flakes in a quartz tube for vacuum sealing, heated to 1000 °C in a box-type electric furnace for 8 h, and then water-cooled and quenched. The alloys with a thickness of 3 mm were rolled to 1.5 mm using a cold-rolled strip experimental rolling mill. The reduction in a single pass was 0.05 mm. Subsequently, the rolled samples were kept at 800 °C for 2 h and then cooled and annealed in the furnace. This allowed the formation of the maximum number of effective strengthening phases in the alloy, which improved the mechanical properties.

Bruker D8 FOCUS X-ray diffractometer (XRD) was used to analyze the phase structure of the rolled surface of the samples. The scanning angle was 20–100° 2θ, and the scanning speed was 10°/min. The sample dimensions were 5 μm in length, 3 μm in width, and 50 nm in thickness. The room temperature tensile experiment was performed on a CMT4105 electronic universal testing machine with a strain rate of 5×10^{-4}/s. The tensile specimens were fabricated in a dog-bone shape along the rolling direction, with a gauge length of 20 mm, a width of 2 mm, and a thickness of 1.5 mm. For the high-temperature tensile experiment, we used an MTS Landmark type high-temperature tensile testing machine. In the experiment, when the samples' surface reached the target temperature, the samples were held for 5 min before stretching, and the strain rate was 5×10^{-4}/s. The performance indicators specified in the high-temperature tensile experiment were the same as those in the room temperature tensile experiment.

3. MD model and method

In this study LAMMPS [16], molecular dynamics simulation software was used to realize the MD simulation calculations of CoCrFeNi $(Al_{0.3}Ti_{0.2})_x$ HEAs x = 0.25, 0.5,0.75,1.00. Fig. 1 shows the CoCrFeNi $(Al_{0.3}Ti_{0.2})_x$ alloy models of different components. In those simulations, the atomic interactions of the Co–Cr–Fe–Ni were described by many-body embedded-atom potential [17,18]. The Ti–Al interactions were described by the empirical embedded-atoms method (EAM) potential [19],. Lennard-Jones potential and Lorenz-Berthelot mixing rules [20,21] were used to describe the remaining atomic interactions, including Co, Cr, Fe, Ni, and Ti and Al. According to the lattice parameters of these single elements, we chose the maximum value of the lattice parameter to build up the initial MD model of CoCrFeNi $(Al_{0.3}Ti_{0.2})_x$. The six elements were randomly distributed in the FCC crystal structure according to the required ratio. As shown in Fig. 1, there are 82944 atoms in the models, with the size of the models being $24a \times 24a \times 36a$ (a is the lattice constant).

In the MD simulations, the periodic boundary conditions have been used in x-, y-, and z-directions. Before the model was loaded, the energy was minimized, and the geometric structure was optimized using a conjugate gradient algorithm. The entire model underwent full relaxation for an isothermal and isostatic pressure (NPT) system to simulate the melting-cooling process. The scalar external pressure is 0 Bar and the pressure damping parameter is 10.0 ps. All atoms were heated to 3000 K at a rate of 1.35 K/ps and relaxed for a while at this temperature to reach equilibrium. The time for equilibration at 3000K is 500 ps. Then, the temperature of the system was reduced at a rate of 0.225 K/ps and relaxed 500ps at 300K. Our cooling rate is below a critical value of 0.333 K/ps as pointed in our previous work [21]. The time-step was set to be 0.001 ps. The Verlet leapfrog method was used to solve the MD integral equation, and the Nose-Hoover thermal bath method was used to control the system temperature. During the loading process, the pressure in the other two directions was always set to zero except for the z-direction where the deformation was applied. Under the NPT system, the model loading process was realized by using a strain rate of 4×10^8 s^{-1} in the simulations.

The visual tool OVITO [22] was used for structural analysis and processing. After relaxation, the simulated powder X-ray diffraction (XRD) patterns were used [23] to analyze the phase structure of the CoCrFeNi$(Al_{0.3}Ti_{0.2})_x$ HEA film [24,25]. The dislocation extraction algorithm (DXA) was employed to analyze the dislocation evolution [26].

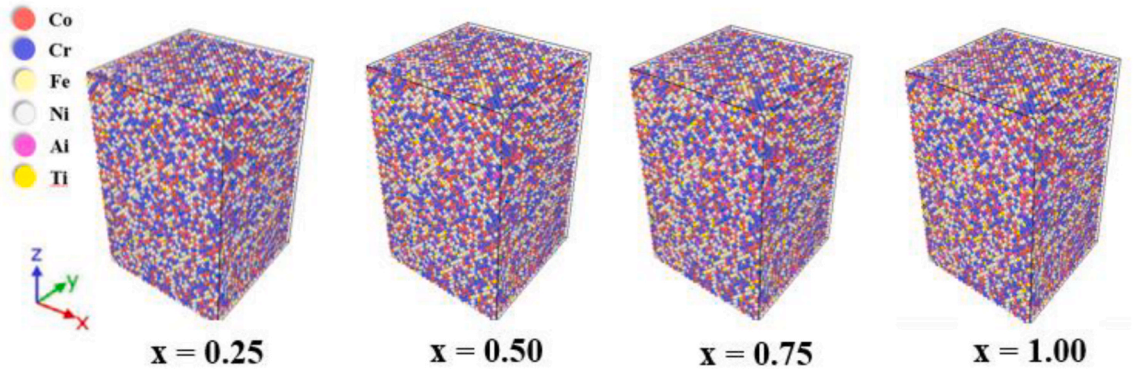

Fig. 1. CoCrFeNi$(Al_{0.3}Ti_{0.2})_x$ HEA models with different Ti and Al contents for x = 0.25, 0.5,0.75,1.00.

4. Results and discussion

4.1. Phase structure

Fig. 2a shows the X-ray diffraction pattern of the CoCrFeNi $(Al_{0.3}Ti_{0.2})_x$ HEA samples after rolling. The CoCrFeNi$(Al_{0.3}Ti_{0.2})_x$ HEA retains its dual-phase structure composed of the FCC matrix phase and γ′ phase with the increase of Ti and Al contents, and other phases are not formed. The γ′ phase has Ni_3(Al, Ti) molecular formula and a face-centered cubic crystal structure of $L1_2$. The γ′ phase forms because the crystal structure of Ni–Al and Ti bonds preferentially appears in the alloy, exhibiting strong chemical order, when Ti and Al alloying elements are added to CoCrFeNi. Conclusively, the XRD results show that micro-additions of Ti and Al elements cause the formation of the γ′ phase in the alloy, which significantly improves the alloy properties through precipitation strengthening methods.

Fig. 2b shows the XRD patterns obtained by MD simulations after the relaxation of the alloy models. The simulation results are consistent with experiment. The HEA exhibits a single FCC phase without apparent second phase peaks. The position of each FCC peak in the XRD pattern shifts toward smaller 2θ angles with the increase of Ti and Al contents. Ti and Al atoms have a large radius in the FCC matrix, causing the lattice distortion. This increases the interplanar spacing, d, so the diffraction peak angle of the matrix decreases. Note that only FCC phase is displayed in Fig. 2b to avoid overlapping with the γ′ phase.

It is worth noting that it is impossible to compare the intensity and width of the XRD peaks of the experimental and simulated samples directly. The relative intensity of the XRD peaks is related to the crystallinity of the material, while the half-width depends on the size of the crystal domain. Hence, the total number of atoms involved in diffraction is entirely different [25].

4.2. Effects of Ti and Al contents

Fig. 3a shows the stress-strain tensile curves of the CoCrFeNi $(Al_{0.3}Ti_{0.2})_x$ HEA at room temperature. With the addition of Ti and Al alloying elements, the yield strength and tensile strength of CoCrFeNi $(Al_{0.3}Ti_{0.2})_x$ HEA gradually increase, as shown in Table 1. Combining the XRD and (S)TEM results, the tensile properties of the alloys could be explained as follows: the increase in the strength of HEAs is attributed to the strengthening of lattice distortion caused by the large atomic radii of Ti and Al elements and the precipitation strengthening of γ′ phase. However, the formation of the γ′ phase reduces the relative content of the plastic FCC matrix in the alloy, resulting in a toughness decrease. Therefore, when the content of Ti and Al increases to x = 1, the strength and toughness of the alloy decrease, and the fracture mechanism of the alloy changes from plasticity to brittleness.

Fig. 3b shows the stress-strain curves obtained by tensile simulation of the CoCrFeNi$(Al_{0.3}Ti_{0.2})_x$ HEA model at a temperature of 300 K and a strain rate of 0.0004 ps^{-1}. The CoCrFeNi$(Al_{0.3}Ti_{0.2})_x$ HEA undergoes the three stages of elasticity-plasticity-fracture. In the first stage, the HEA follows Hookean's law, and the elastic modulus of the alloy can be obtained by linear fitting of the slope in the elastic stage. With the strain increase, the HEA enters the plastic stage, and the stress-strain curves of the alloy change nonlinearly. The rapid drop in stress-strain curve after the maximum indicates that the alloy has experienced a fractured failure. The peak stress in the curves represents the tensile strength of the alloy. Table 1 lists the elastic modulus and tensile strength of the

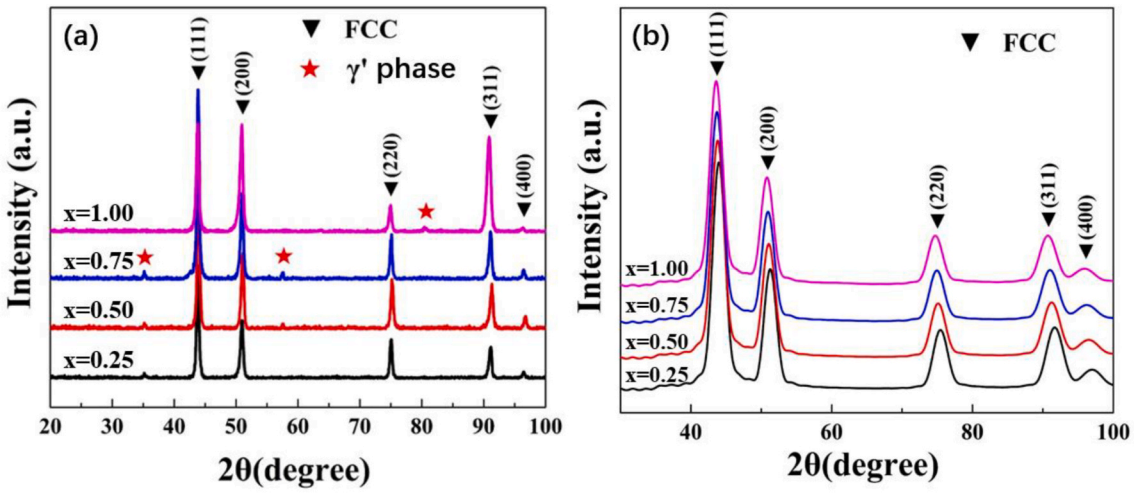

Fig. 2. XRD patterns of the CoCrFeNi$(Al_{0.3}Ti_{0.2})_x$ HEA after rolling: (a) experiment; and (b) MD simulations.

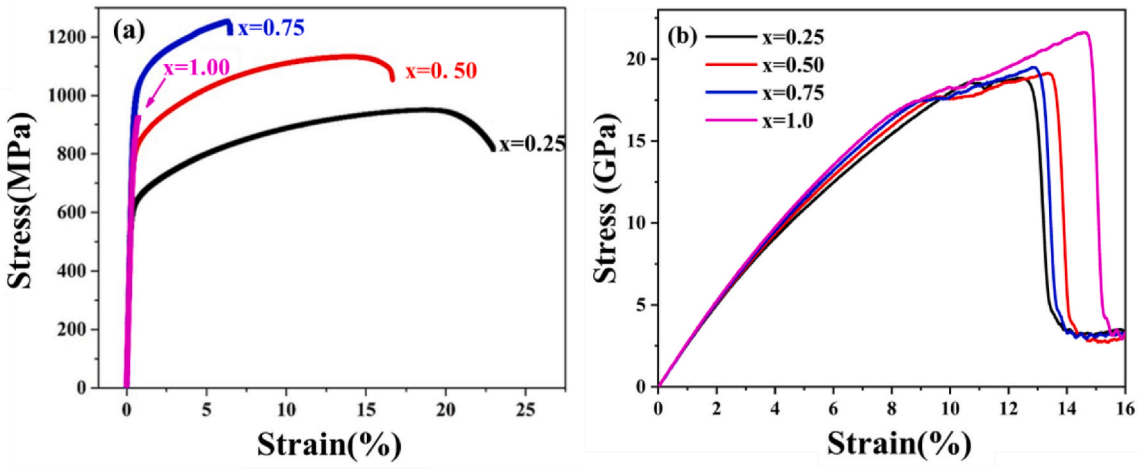

Fig. 3. Stress-strain tensile characteristics of the CoCrFeNi$(Al_{0.3}Ti_{0.2})_x$ HEA: (a) experimental stress-strain curves at room temperature and (b) MD simulated tensile stress-strain curves.

Table 1
Tensile mechanical properties of the CoCrFeNi$(Al_{0.3}Ti_{0.2})_x$ HEA at room temperature.

High-entropy alloy	Experiments			MD simulations	
	yield strength/ MPa	tensile strength/ MPa	tensile elongation/ %	elasticity modulus/ GPa	tensile strength/ GPa
x = 0.25	616.9	951.1	24.7	171.9	18.8
x = 0.50	808.0	1132.6	18.3	184.5	19.1
x = 0.75	1029.2	1250.8	7.2	194.1	19.5
x = 1.00	875.1	889.2	0.4	205.6	21.6

CoCrFeNi$(Al_{0.3}Ti_{0.2})_x$ HEA tensile simulation. With the increase of Ti and Al contents, the elastic modulus and tensile strength increase, indicating that the alloy's stiffness enhances while the toughness becomes worse.

During the stretching process, as the grains of the stretched CoCrFeNi $(Al_{0.3}Ti_{0.2})_x$ HEA undergo deformation, the dislocations move inside the material, increasing the dislocation density [27,28]. Fig. 4 shows dislocation distribution diagrams of the CoCrFeNi$(Al_{0.3}Ti_{0.2})_x$ HEA before fracturing. With the increase of Ti and Al contents, the dislocation density of the HEA significantly increases, leading to an intensified dislocation intersect. This causes an increase in deformation resistance and makes difficulties for the continued plastic deformation, thereby increasing the deformation resistance of the alloy.

4.3. Effect of temperature

According to the mechanical performance at room temperature in the previous section, the overall performance of the CoCrFeNi $(Al_{0.3}Ti_{0.2})_x$ HEA was optimal when x = 0.75. Therefore the CoCrFeNi$Al_{0.225}Ti_{0.15}$ HEA was selected for the high-temperature tensile experiments. The experimental temperatures were 400, 500, and 650 °C. Fig. 5 shows the yield strength, tensile strength, and elongation at different temperatures. When the tensile temperature is 400 °C, the yield strength, tensile strength, and elongation of the CoCrFeNi$Al_{0.225}Ti_{0.15}$ HEA are 837.0 MPa, 1077.1 MPa, and 12.9%, respectively. When the tensile temperature exceeds 500 °C, the decrease rate of the HEA strength increases, and the yield strength, tensile strength, and elongation are 796.7 MPa, 1059.8 MPa, and 13.7%. At 650 °C, the yield strength and tensile strength of the CoCrFeNi$Al_{0.225}Ti_{0.15}$ HEA decrease to 594.8 and 791.2 MPa, respectively, while the elongation increases slightly to 15.2%.

Fig. 6 shows the tensile simulation of the CoCrFeNi$(Al_{0.3}Ti_{0.2})_x$ HEA models with a strain rate of 0.0004 ps^{-1} at different temperatures. The mechanical properties of CoCrFeNi$(Al_{0.3}Ti_{0.2})_x$ HEA exhibit a strong temperature dependence. When the system temperature rises from 300 to 873 K, the HEA models with different Ti and Al contents undergo the same three stages of elasticity-plasticity-fracture. The overall trends of the stress-strain curves are consistent. With the further temperature increase, the model's elastic modulus and tensile strength with the same composition show a decreasing trend, which is consistent with the experimental results.

Fig. 6 also represents the dislocation distribution of the CoCrFeNi

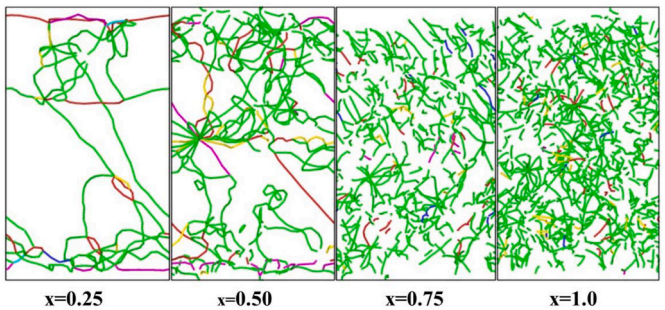

Fig. 4. Dislocation distribution diagrams before the fracture in the CoCrFeNi $(Al_{0.3}Ti_{0.2})_x$ HEA.

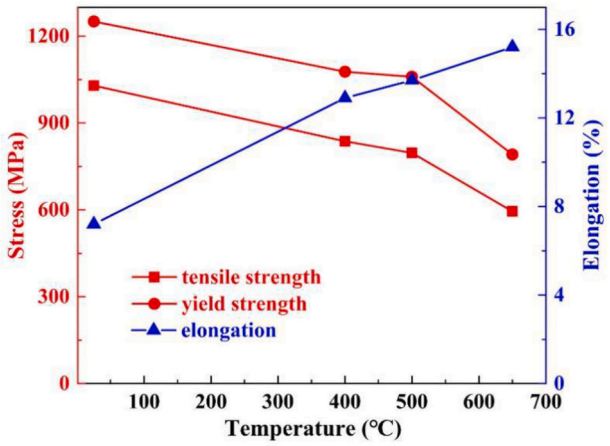

Fig. 5. The tensile mechanical properties of the CoCrFeNi$(Al_{0.3}Ti_{0.2})_{0.75}$ HEA experimentally determined at 400, 500, and 650 °C.

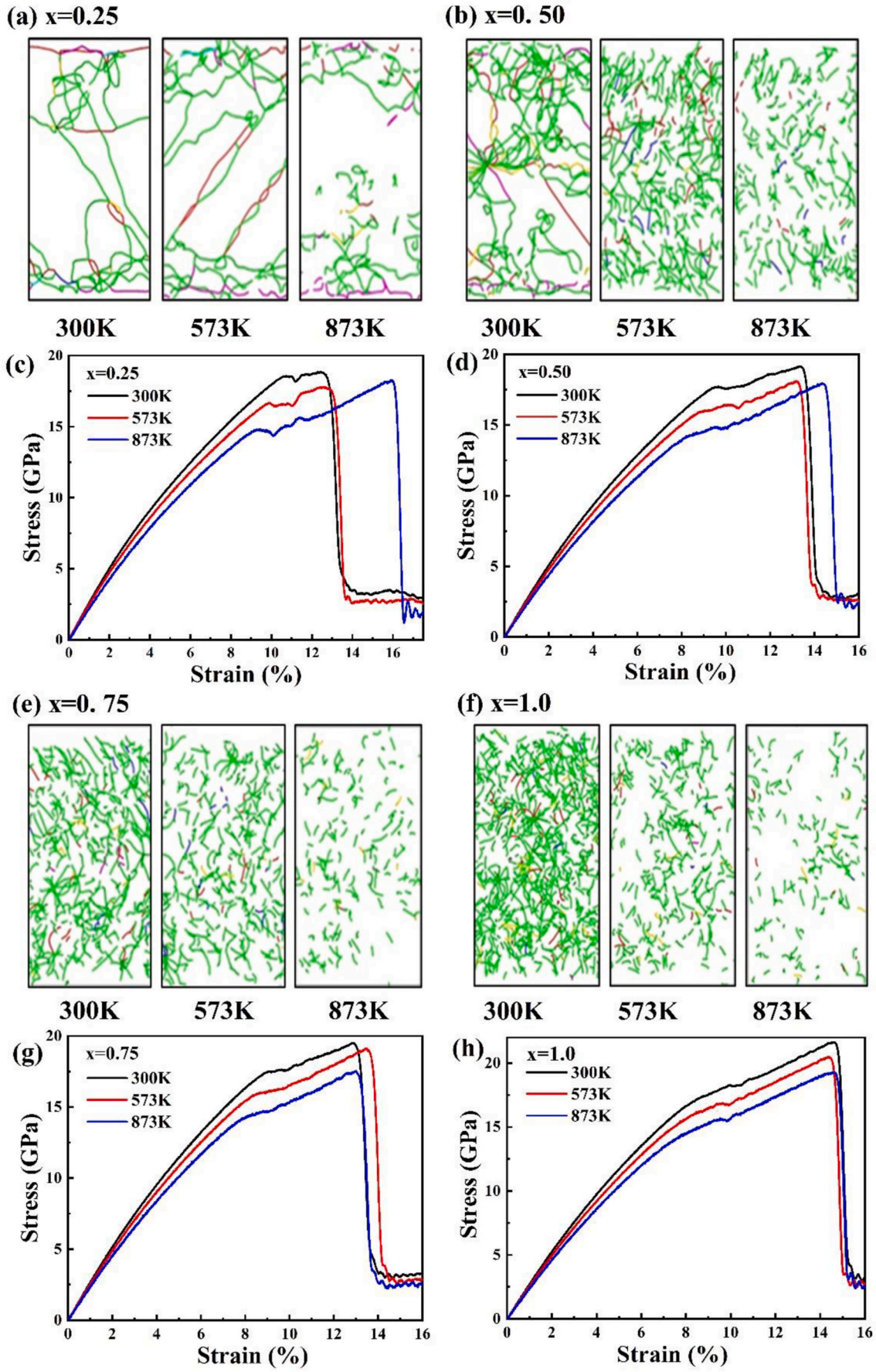

Fig. 6. Simulation of the CoCrFeNi$(Al_{0.3}Ti_{0.2})_x$ HEA tensile stress-strain curves and dislocation distributions before fracturing at 300, 573, and 873 K.

$(Al_{0.3}Ti_{0.2})_x$ HEA before fracturing at different temperatures. As the temperature increases, the dislocation density before the alloy fracture significantly decreases. The reason for this phenomenon is that the increase in deformation temperature leads to a larger cell size, which in turn reduces the dislocation density [29]. As the temperature reaches a certain level, the dislocations overcome some short-range energy barriers through the thermal activation energy provided by the system and thus, reduce the dislocation transport, which in turn decreases the tensile strength of the alloy.

It is worth mentioning that molecular dynamics suffers from the limitations including the short time scale (<μs), small system size (<μm), over-simplified model, and relatively inaccurate interatomic interactions. Therefore, it is well known that the results of MD simulations agree qualitatively with experiment. The strain rates in MD simulations in general are several orders of magnitude higher than that in the real experiment. Despite the difference in strain rate due to the intrinsic limitations of the method, molecular dynamics is valuable to model the system from the micro and nano scales for various information and applications.

5. Conclusions

$CoCrFeNi(Al_{0.3}Ti_{0.2})_x$ HEA has been successfully prepared by vacuum arc melting using CoCrFeNi alloy as a matrix and adding Ti and Al trace elements to tailor the HEA composition. We have used XRD to investigate the phase structure of the prepared samples. HEAs' mechanical properties with different compositions have been assessed using room temperature tensile experiments, and the $CoCrFeNiAl_{0.225}Ti_{0.15}$ HEA with the optimal room temperature mechanical performance was selected for the high-temperature tensile experiments. Besides, the MD method was used to establish the $CoCrFeNi(Al_{0.3}Ti_{0.2})_x$ HEA model and perform an XRD simulation analysis of its structure. Micromechanical properties of the HEA at different Ti and Al contents and temperatures were also calculated. The main conclusions are as follows:

(1) Using XRD experimental method, we have investigated the alloys' phase composition. $CoCrFeNi(Al_{0.3}Ti_{0.2})_x$ alloys were mainly composed of the FCC matrix phase and γ′ phase $Ni_3(Al, Ti)$, which proved that the micro-additions of Ti and Al caused the formation of high-temperature strengthening phases in the CoCrFeNi HEA. The positions of the main diffraction peaks in the MD simulation were consistent with the experiment. With the increase of Ti and Al contents, the diffraction peaks shifted toward smaller 2θ angles, which is related to the alloy lattice distortion.

(2) The results of tensile experiments at room temperature showed that with the continuous addition of Ti and Al alloying elements, the yield strength and tensile strength of the CoCrFeNi $(Al_{0.3}Ti_{0.2})_x$ HEA gradually increases, while the elongation gradually decreases. However, when the content of Ti and Al is increased to $x = 1$, the plastic fracture mechanism shifts to the brittle fracture mechanism. The MD tensile simulation results can be summarized as follows: with the increase of the Ti and Al contents, the elastic modulus and tensile strength of the HEA increased continuously, while the tensile strength increased with the dislocation density.

(3) By studying the high-temperature mechanical properties of the $CoCrFeNiAl_{0.225}Ti_{0.15}$ HEA, as the temperature of the tensile stretching is increased, the strength of the HEA gradually decreases, but the toughness increases. The MD tensile simulation results at different temperatures also show that HEAs' elastic modulus decreases with the temperature. The dislocation distribution before the HEA fracture confirms that the dislocation density in the HEA gradually reduces with the tensile experiment temperature, leading to a decrease in tensile strength.

CRediT authorship contribution statement

Zhi Hui Sun: Data curation, Writing – original draft. **Jie Zhang:** Data curation, Writing – original draft, Visualization, Software, Investigation. **Gao Xin Xin:** Visualization, Software, Investigation. **Lu Xie:** Conceptualization, Methodology, Supervision, Project administration, Validation. **Li Chun Yang:** Investigation, Resources. **Qing Peng:** Supervision, Writing – review & editing.

Declaration of competing interest

The authors declare that they have no known competing financial interests or personal relationships that could have appeared to influence the work reported in this paper.

Acknowledgements

This work was supported by the National Key R&D Program of China (Grant No. 2020YFA0405700) and the Fundamental Research Funds for the Central Universities (Grant No. FRF-MP-20-31). Q. P. would like to acknowledge the support provided by LiYing Program of the Institute of Mechanics, Chinese Academy of Sciences (Grant No. E1Z1011001).

References

[1] J.W. Yeh, et al., Nanostructured high-entropy alloys with multiple principal elements: novel alloy design concepts and outcomes, Adv. Eng. Mater. 6 (5) (2004) 299–303.
[2] J. Ding, et al., Tunable stacking fault energies by tailoring local chemical order in CrCoNi medium-entropy alloys, Proc. Natl. Acad. Sci. Unit. States Am. 115 (2018) 201808660.
[3] Q.J. Li, H. Sheng, E. Ma, Strengthening in multi-principal element alloys with local-chemical-order roughened dislocation pathways, Nat. Commun. 10 (1) (2019).
[4] W. Chen, et al., Alloying behavior, microstructure and mechanical properties in a FeNiCrCo0.3Al0.7 high entropy alloy, Mater. Des. 51 (2013) 854–860.
[5] M.H. Chuang, et al., Microstructure and wear behavior of AlxCo1.5CrFeNi1.5Tiy high-entropy alloys, Acta Mater. 59 (16) (2011) 6308–6317.
[6] J.-W. Yeh, et al., Anomalous decrease in X-ray diffraction intensities of Cu–Ni–Al–Co–Cr–Fe–Si alloy systems with multi-principal elements, Mater. Chem. Phys. 103 (1) (2007) 41–46.
[7] S.G. Ma, et al., Superior high tensile elongation of a single-crystal CoCrFeNiAl0.3 high-entropy alloy by Bridgman solidification, Intermetallics 54 (2014) 104–109.
[8] T.T. Shun, Y.C. Du, Microstructure and tensile behaviors of FCC Al 0.3 CoCrFeNi high entropy alloy, J. Alloys Compd. 479 (1–2) (2009) 157–160.
[9] J.Y. He, et al., A precipitation-hardened high-entropy alloy with outstanding tensile properties, Acta Mater. 102 (2016) 187–196.
[10] Y. Dong, et al., Microstructure and mechanical properties of AlCoxCrFeNi3-x eutectic high-entropy-alloy system, J. Alloys Compd. (2020) 823.
[11] Q. Peng, F. Meng, Y. Yang, C. Lu, H. Deng, L. Wang, S. De, F. Gao, Shockwave generates < 100 > dislocation loops in bcc iron, Nat. Commun. 9 (1) (2018) 4880, 4880.
[12] Liu, et al., Mechanical behaviors of AlCrFeCuNi high-entropy alloys under uniaxial tension via molecular dynamics simulation, RSC Adv. (2016).
[13] Y, et al., Tensile Properties of AlCrCoFeCuNi Glassy Alloys: A Molecular Dynamics Simulation Study, Materials Science & Engineering A, 2017.
[14] A.V. Korchuganov, Onset of plastic deformation in non-equiatomic fcc CoCrFeMnNi high-entropy alloys under high-rate loading, Lett. Mater. 8 (3) (2018) 311–316.
[15] Y. Qi, Zhaomin, M. Feng, Molecular simulation of microstructure evolution and plastic deformation of nanocrystalline CoCrFeMnNi high-entropy alloy under tension and compression, J. Alloys Compd. (2020) 851.
[16] S. Plimpton, Fast Parallel Algorithms for Short-Range Molecular Dynamics, 1995.
[17] M.S. Daw, S.M. Foiles, M.I. Baskes, The embedded-atom method: a review of theory and applications, Mater. Sci. Rep. 9 (7–8) (1993) 251–310.
[18] X. Zhou, R. Johnson, H. Wadley, Misfit-energy-increasing dislocations in vapor-deposited CoFe/NiFe multilayers, Phys. Rev. B 69 (14) (2004) 144113, 0.
[19] R.R. Zope, Y. Mishin, Interatomic potentials for atomistic simulations of the Ti-Al system, Phys. Rev. B 68 (2) (2003) 366–369.
[20] Imafuku, et al., Computer simulations of the structures of the metallic superlattices Au/Ni and Cu/Ni and their elastic moduli, J. Phys. F Met. Phys. (1986).
[21] L. Xie, et al., AlCoCrCuFeNi high entropy alloy cluster growth and annealing on silicon: a classical molecular dynamics simulation study, Appl. Surf. Sci. 285 (2013) 810–816.
[22] Alexander, Stukowski, Visualization and Analysis of Atomistic Simulation Data with OVITO–The Open Visualization Tool, Modelling & Simulation in Materials Science & Engineering, 2010.

[23] S.P. Coleman, D.E. Spearot, L. Capolungo, Virtual diffraction analysis of Ni [010] symmetric tilt grain boundaries, Model. Simulat. Mater. Sci. Eng. 21 (5) (2013) 55020.
[24] A. Kazakov, E. Shpiro, T. Voskoboinikov, Application of debye function analysis to particle size and shape determination in Ir/SiO2 catalysts, J. Phys. Chem. 99 (1995).
[25] L. Xie, et al., Molecular Dynamics Simulation of Al–Co–Cr–Cu–Fe–Ni High Entropy Alloy Thin Film Growth, Intermetallics, 2016.
[26] A. Stukowski, V.V. Bulatov, A. Arsenlis, Automated identification and indexing of dislocations in crystal interfaces, Model. Simulat. Mater. Sci. Eng. 20 (8) (2012) 85007.
[27] J. Liu, G. Zhu, W. Mao, S.V. Subramanian, Modeling of critical grain size for shifting plasticity enhancement to decrease by refining grain size - ScienceDirect, Mater. Sci. Eng., A 607 (1) (2014) 302–306.
[28] L.P. Evers, W.A.M. Brekelmans, M.G.D. Geers, Scale dependent crystal plasticity framework with dislocation density and grain boundary effects, Int. J. Solid Struct. 41 (18–19) (2004) 5209–5230.
[29] M.R. Staker, D.L. Holt, The dislocation cell size and dislocation density in copper deformed at temperatures between 25 and 700°C, Acta Metall. 20 (4) (1972) 569–579.